PHYSICAL REVIEW B VOLUME 39, NUMBER 15 15 MAY 1989-II

Mesoscopic properties of on-facet $Al_xGa_{1-x}As/GaAs$ submicron channels

Syoji Yamada
Nippon Telegraph and Telephone Corporation Laboratories, 3-9-11, Midoricho, Musashino-shi, Tokyo 180, Japan

Hiromitsu Asai
Nippon Telegraph and Telephone Corporation Opto-Electronics Laboratories, 3-1 Morinosato Wakamiya, Atsugi-shi, Kanagawa 243-0, Japan

Yoshino K. Fukai and Takashi Fukui
Nippon Telegraph and Telephone Corporation Laboratories, 3-9-11, Midoricho, Musashino-shi, Tokyo 180, Japan
(Received 25 January 1989)

Mesoscopic properties of on-facet $Al_xGa_{1-x}As/GaAs$ submicron channels are reported. These channels are buried at facet interfaces by subsequent selective growth in metalorganic chemical vapor deposition. From basic estimations, including positive magnetoconductance analysis, several features such as a very thin depletion layer and a small negative-power temperature dependency of inelastic scattering length are noted. Reproducible conductance fluctuations (CF's) are also observed. By use of spectrum-analysis results of the CF's, a competition between backward-interference modes observed in a oblique double-channel configuration is discussed.

To study the novel physics expected in small-sized devices, various mesocopic systems based on metals[1] and/or semiconductors such as GaAs[2,3] and Si-metal-oxide-semiconductor (Si-MOS)[4-6] have been investigated. Recently, quantum wires and rings[7-11] based on planar $Al_xGa_{1-x}As/GaAs$ two-dimensional electron gas (2D EG) structures have revealed good qualities such as long inelastic and elastic scattering lengths, even after sophisticated fabrication processes. By utilizing these merits, some new phenomena, for example, quantized conductance of 2D EG point contacts,[12] have recently been reported. However, there are also some disadvantages, such as precarious side depletion and degradation of electronic properties, since these structures are usually fabricated with electron-beam or focused-ion-beam lithographies, and hence are not free from damage and/or contamination.

Recently we demonstrated[13] narrow 2D EG channels fabricated on $Al_xGa_{1-x}As/GaAs$ facet interfaces as novel candidates for mesoscopic systems. Since this channel is fabricated by subsequent selective growth in the metalorganic chemical vapor deposition (MOCVD) method and hence is *buried* at facet interfaces, it can eliminate the disadvantages described above. In addition, a variety of channel configurations can be realized. This is interesting in relation to novel device applications.

In this work, we report the first experimental study of interference effects in such channels having submicron widths. Some basic features unique to these channels are described initially. Then a mode competition phenomenon, observed in the spectral analysis of conductance fluctuations (CF's), is discussed.

Cross-sectional views of mesa-shaped bars containing 2D EG channel(s) are shown in Fig. 1. The SiO_2 mask has multiple 1-μm wide windows in periods of 2–10 μm in the [110] direction on a semi-insulating GaAs substrate. The GaAs mesa-shaped bar is first grown and then covered by about a 0.01-μm-thick spacer and a 0.1-μm-thick Si-doped $Al_xGa_{1-x}As$ layer. Two different channel configurations are obtained. The 2D EG is located on the top-(001) interface in type *A* and is on both the sidewall-{111}*A* interfaces in type *B*. The channel width *W* is controlled mainly by the width of the mask window in type *A*, and by the GaAs layer thickness in type *B*. Fabrication control for these two types of configurations is carried out by selecting several growth conditions such as growth temperature, gas partial pressure, period of the mask, etc. In particular, the anisotropy of the $Al_xGa_{1-x}As$ growth rate on {111}*A* and on (001) GaAs surfaces varies with those conditions. Consequently, the thickness of $Al_xGa_{1-x}As$ (spacer and Si doped) layers and the segregation coefficient of Si dopant become different. Under certain conditions, the hybrid structure in which type *A* and type *B* are partially combined is obtained. The mechanisms involved are not yet perfectly understood; hence, the details of the fabrication process will be discussed in the future. The buried channels obtained at facet interfaces are referred to here as *on-facet* 2D EG channels or quantum wires. Two-terminal devices with channel lengths of 1–50 μm were fabricated using the usual photolithographic technique. A single mesa-shaped-bar sample was obtained through a lithographic process or by a focused Ga-ion-beam implanation which yields high-resistivity regions in the unnecessary channels.

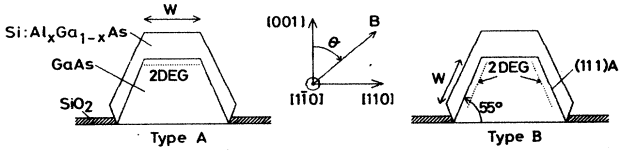

FIG. 1. Cross-sectional views of a mesa-shaped bar containing on-facet 2D EG channel(s).

Several fundamental properties of the three measured samples are listed in Table I. The 2D EG location and the sheet electron density n_s were determined from the angular-dependent Shubnikov–de Haas (SdH) oscillations.[13] The peak fields are confirmed to vary by $1/\cos\theta$ and $1/\cos(\theta \pm 55°)$ in type A and type B, respectively. Here θ is the deviation angle of magnetic field B from the [001] direction toward the [110] direction (see Fig. 1). Since 0° and $\mp 55°$ are the angles when B is normal to (001) and $\{111\}A$ facets, respectively, these results clearly indicate that the 2D EG exists only on the (001) facet in type A and the $\{111\}A$ facets in type B. Localization dimension and mobility μ were estimated from zero magnetic field conductance $\sigma(B=0)$ and n_s. High μ with large n_s is one feature of our channels. The 2D EG's in these samples were found to occupy the ground and the first-excited subband. The higher μ in type A than in type B probably originates from the shorter interruption time between the GaAs and $Al_xGa_{1-x}As$ growth processes. As the interruption time becomes longer, the facet interface may be degraded and the number of impurities self-doped at the interface may increase. The large n_s may also be attributed partly to such impurities. Low-field magneto conductance (MC) measurement in two-terminal devices was carried out by the conventional ac lock-in method at 190 Hz at temperatures of 1.4–40 K. The sample current was less than 10 nA.

In long multiple mesa-shaped-bar samples, inelastic scattering length L_i was estimated on the basis of positive MC's. The samples used had the following dimensions: for A-1, $W=0.3$ μm (×20 lines), $L=50$ μm; for B-1, $W=0.6$ μm (×30 lines), $L=20$ μm. A fitting theory was selected with the localization dimension determined from the temperature dependencies of $\sigma(B=0)$. The 1D theory of Dugaev and Khmel'nitskii,[14] which was modified to include the effect of scatterings by channel sidewalls, was used for A-1, while the 2D theory of Hikami, Larkin, and Nagaoka[15] was used for B-1. The raw temperature dependencies of L_i for A-1 and B-1 samples are plotted in Fig. 2 with open symbols (lines a and d). The positive magnetoconductances in various temperatures and the fitting results for the A-1 sample are shown in the inset. Both data (lines a and d) exhibit a small negative power against the temperature, roughly as $T^{-1/4}$. Such small negative power is not, however, explained by the conventional 1D (Refs. 14 and 16) or 2D (Ref. 17) localization theories. Therefore further analyses were carried out for the A-1 sample. First, the effect of parallel conduction was eliminated. Next, the L_i was estimated from the averaged amplitude of temperature-dependent CF's (not shown in this paper) using the equation

$$\Delta G_e = (e^2/h)[\max(L_i, W)/L]^{1/2}(L_i/L) . \quad (1)$$

Here, the single mesa-shaped-bar sample of A-1 in which CF's were observed had dimensions of $W=0.3$ μm and $L=5$ μm. Parallel conduction correction was carried out by subtracting positive MC when the magnetic field angle $\theta=90°$ from that when $\theta=0°$. In Fig. 2, these results are plotted with solid symbols (lines b and c) for comparison.

The temperature dependencies are, however, similar to that of the raw results. This suggests that a small negative power is highly likely and originates from some un-

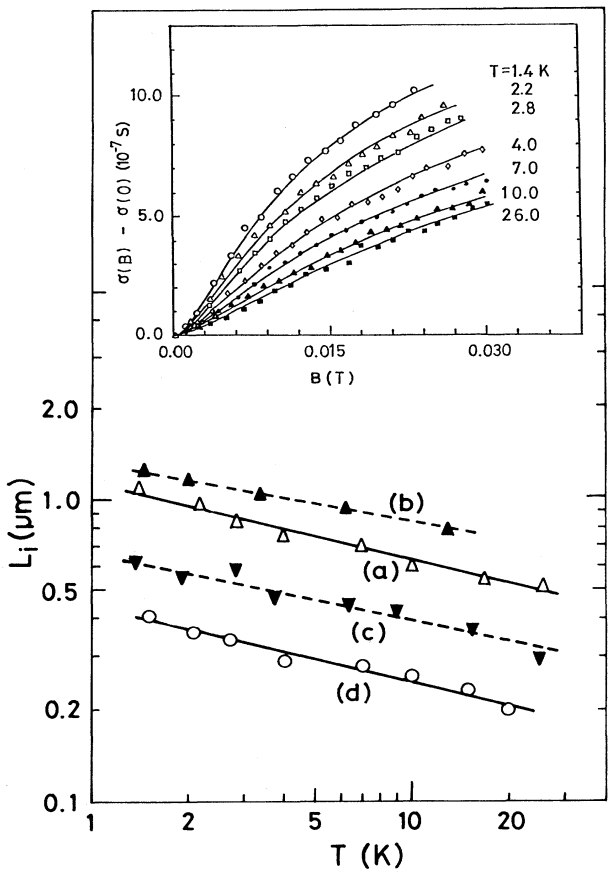

FIG. 2. Typical temperature dependencies of L_i for A-1 and B-1 channels. Line a, raw data for the A-1 sample; line b and c, corrected data for the A-1 sample (see text); line d, raw data for the B-1 sample. Samples used: $W=0.3$ μm×20 lines, $L=50$ μm for A-1; $W=0.6$ μm×30 lines, $L=20$ μm for B-1. The single mesa-shaped-bar sample of A-1 in which CF's were observed in order to estimate L_i had a length of 5 μm. In magnetoconductance measurement, current flow is parallel to the [110] direction under the applied magnetic field in the (110) plane. The inset shows positive magnetoconductances in the A-1 sample at various temperatures which were fitted by 1D localization theory.

TABLE I. Some basic properties of the various on-facet channels. n_s is the sheet electron density; μ is the electron mobility, W_{SEM} is the channel width determined from a SEM photograph; W_{fit} is the channel width determined from a fitting by the weak localization theory; and L_e is the elastic scattering length.

Sample	n_s (10^{12} cm^{-2})	μ (m^2/Vs)	W_{SEM} (μm)	W_{fit} (μm)	L_e (μm)
A-1	3.46	3.4	0.3	0.3	0.7
A-2	1.70	4.2	1.05	1.0	0.5
B-1	1.75	0.6	0.64	0.6	0.1

known phase-breaking factors in the measured temperture range. Thus the temperature dependencies of L_i's are roughly determined as $0.85T^{-0.2}$ and $0.45T^{-0.25}$ (uncorrected) for the A-1 and B-1 samples, respectively. The 1D-2D crossover ($L_i = W$) temperature is therefore ≥ 10 K for A-1 and about 1 K for B-1. The reason for the small negative power is not clear at present but there are at least two possibilities. One is that the small power dependency may be part of a saturation over a wide temperature range. Since spin-spin or spin-orbit scattering is probably not the origin for the saturation, inelastic interface scattering or Joule heating could be responsible. Another possible reason is the large n_s in our channels. Indeed one parameter used in the fitting theory[18] was found to depend on n_s, suggesting a close relation between L_i and n_s. Electron-electron interaction, which acts as a dominant inelastic scattering source, may be modified in our case. Experiments in a wider temperature range are now under way. Further discussion will be provided in the future.

The differences between the channel widths determined from the fittings W_{fit} and those from scanning electron microscope (SEM) photograph W_{SEM} are as small as 0.05 μm. The fact that it is almost unnecessary to consider the effect of side depletion is one advantage of on-facet channels. This promotes easy design of mesocopic devices based on one-facet channels. It is also found that the transport regime of A-2 and B-1 is diffusive ($L_e \leq W \leq L$) while that of A-1 is quasiballistic ($W \leq L_e \leq L$). The latter suggests dominance of specular boundary scattering,[11] reflecting the good quality of the A-1 channel.

In the short single mesa-shaped-bar samples, reproducible conductance oscillations were observed. The angular dependencies of the oscillation for the A-1 and B-1 samples are shown in Figs. 3(a) and 3(b). The expected fluctuation magnitudes ΔG_e estimated by Eq. (1) are $0.064(e^2/h)$ for A-1 and $0.38(e^2/h)$ for B-1. These are also indicated in Fig. 3 and almost coincide with the experimental results. The CF's roughly depend on the angle θ of magnetic field B as $1/\cos\theta$ for type A and $1/\cos(\theta - 55°)$ for type B. Here, θ has the same definition as in the SdH observations. Therefore, these two kinds of dependencies suggest that the main origin of each oscillation is the 2D EG on the top or the side-wall interface(s). The ambiguity in these angular-dependent CF's may come from the bulky parallel conduction coexisting with 2D EG and the mode competition, especially in the case of the B-1 sample, as described below.

To understand the microscopic interference events underlying the CF's, a spectrum analysis was carried out. Hereafter we focus on the CF's for type B. Unlike in the work by Taylor *et al.*[19] in which CF's in n^+-type GaAs

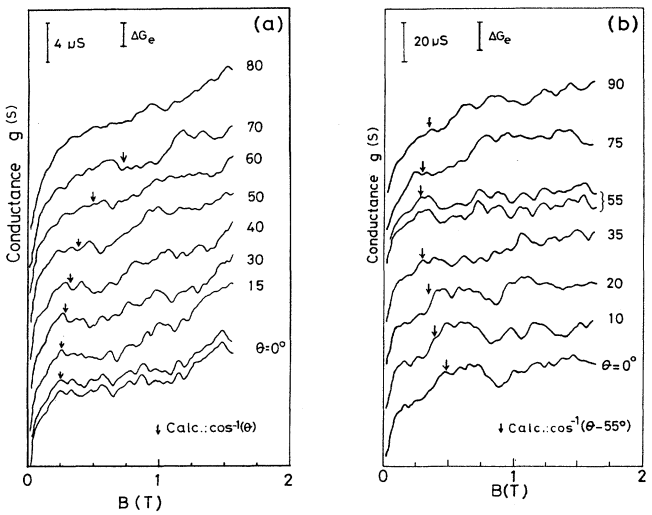

FIG. 3. Angular dependent conductance fluctuations (a) in A-1 chart and (b) in B-1 chart in single mesa-shaped-bar samples. Sample dimensions are $L = 5$ μm and $W = 0.3$ μm for A-1 and $L = 1.1$ μm and $W = 0.6$ μm $\times 2$ for B-1. ΔG_e is the theoretically estimated amplitude of CF's (see text). It corresponds to $0.064(e^2/h)$ for (a) and $0.38(e^2/h)$ for (b). Arrows are the field positions from inverse cosine calculations of $1/\cos\theta$ and $1/\cos(\theta - 55°)$.

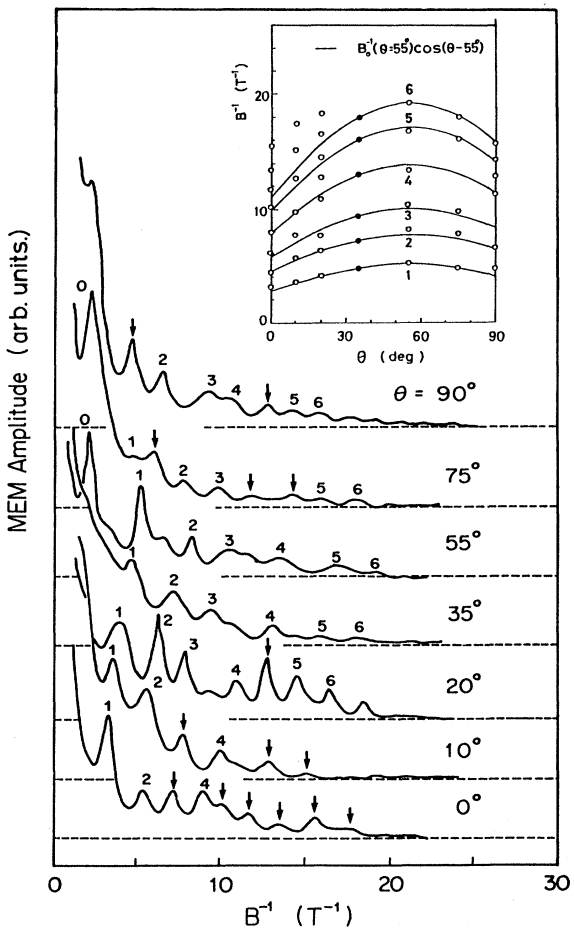

FIG. 4. MEM spectra of the conductance fluctuations shown in Fig. 3(b). The inset is the angular dependency of MEM peak frequency which shows mostly $\cos(\theta - 55°)$ characteristics. The number labels assigned to the MEM peaks are tentative ones. The peaks which are not explained by the cosine calculation are indicated by arrows.

wire were analyzed by FFT (fast Fourier transform), we have adopted a novel spectrum analysis tool—*maximum entropy method* (MEM).[20] This is a nonlinear method which approximates a probability process by an autoregressive model. This makes it possible to determine the correct spectrum from short-length (when compared with the period) data. Also the resolution of spectrum in MEM is very high. Since the field range of CF observed in (on-facet) 2D EG narrow channels is usually restricted in the low field, a more reliable spectrum, suitable for quantitative discussion, can be obtained by MEM than by FFT.

Figure 4 shows the MEM spectra of the CF's shown in Fig. 3(b). In each spectrum, there are at most ten peaks, each corresponding to different sized backward interference loops.[19] These spectra are true, since frequencies of all peaks are found to be fixed even if the temperature is raised.[19] However, they should shift with $\cos(\theta-55°)$ when θ is varied. This is confirmed in the inset, in which $1/B$ peak frequencies for various angles are compared with the cosine calculations based on the $\theta=35°$ data. At this angle, B penetrates only one side channel, since it is parallel to another side channel. The spectrum at $\theta=35°$, therefore, contains interference modes only from the one side channel. Thus, all the spectrum peaks can be tentatively labeled as shown in the figure. However, there are several peaks (as indicated by arrows in the figure) which deviate from the calculation. These are interference modes occurring in another side channel. When θ approaches 0° (and 90°), *competition* between interference events from both channels can easily occur. In other words, the channel in which a certain interference mode occurs can be specified. One- or two-channel situations can be *effectively* realized depending on the angle θ of B. When $\theta\sim35°$–$55°$, the sample effectively behaves as if it contained only one channel. At $\theta\sim0°$ and 90°, the interference events take place in both channels. However, in that case, interference events having equal frequencies do not occur in both channels; that is, there is a *competition* of modes. This originates from the fact that CF is a probability process. This interesting property is possible due to the unique channel configuration (double and oblique to each other) of the type-B sample. This is also one reason for the ambiguity in the angular-dependent CF's described earlier.

We have investigated quantum interference properties of on-facet 2D EG submicron channels, which represent the first realization of a buried-type mesoscopic system. The channels are found to have high mobility with large-sheet carrier density and a very thin side-depletion region. It is also found that inelastic scattering lengths have small negative-power dependencies upon temperature as $\propto T^{-0.25\pm0.05}$ in both 1D and 2D cases. In addition, a fluctuation competition phenomenon between neighboring channels in a unique configuration is found and discussed using spectrum analysis.

The authors thank Dr. Yoshiro Hirayama for cooperation with focused ion-beam work and Professor Shinji Kawaji of Gakushuin University for helpful advice relating to the ac lock-in method. We are also indebted to Dr. Kiyomasa Sugii, Dr. Nobuhiko Susa, and Dr. Tatuya Kimura for their continuous encouragement.

[1]C. P. Umbach, S. Washbern, R. B. Laibowitz, and R. A. Webb, Phys. Rev. B **30**, 4048 (1984).

[2]G. P. Whittington, P. C. Maan, L. Eaves, R. P. Taylor, S. Thoms, S. P. Beaumont, and C. D. W. Wilkinson, Superlattices Microstruct. **2**, 381 (1986).

[3]K. Ishibashi, K. Nagata, K. Gamo, S. Namba, S. Ishida, K. Murase, M. Kawabe, and Y. Aoyagi, Solid State Commun. **61**, 385 (1987).

[4]J. C. Licini, D. J. Bishop, M. A. Kastner, and J. Melngailis, Phys. Rev. Lett. **55**, 2987 (1985).

[5]S. B. Kaplan and A. Hartstein, Phys. Rev. Lett. **56**, 2403 (1986).

[6]W. J. Skocpol, P. M. Mankiewich, R. E. Howard, L. D. Jackel, D. M. Tennant, and A. D. Stone, Phys. Rev. Lett. **56**, 2865 (1986).

[7]K. K. Choi, D. C. Tsui, and K. Aravi, Appl. Phys. Lett. **50**, 110 (1987).

[8]G. Timp, A. M. Chang, P. Mankiewich, R. Behringer, J. E. Cunningham, T. Y. Chang, and R. E. Howard, Phys. Rev. Lett. **59**, 732 (1987).

[9]T. J. Thornton, M. Pepper, H. Ahmed, G. J. Davies, and D. Andrews, Phys. Rev. B **36**, 4514 (1987).

[10]H. van Houten, B. J. van Wees, J. E. Mooji, G. Roos, and K.-F. Berggren, Superlattices Microstruct. **3**, 497 (1987).

[11]H. van Houten, C. W. J. Beenakker, B. J. van Wees, and J. E. Mooji, Surf. Sci. **196**, 144 (1988).

[12]B. J. van Wees, H. van Houten, C. W. J. Beenakker, J. G. Williamson, L. P. Kouwenhoven, D. van der Marel, and C. T. Foxon, Phys. Rev. Lett. **60**, 848 (1988); D. A. Wahram, T. J. Thornton, R. Newbury, M. Pepper, H. Ahmed, J. E. F. Frost, D. G. Hasko, D. C. Peacock, D. A. Ritchie, and G. A. C. Jones, J. Phys. C **21**, L209 (1988).

[13]H. Asai, S. Yamada, and T. Fukui, Appl. Phys. Lett. **51**, 1518 (1987).

[14]V. K. Dugaev and D. E. Khmel'nitskii, Zh. Eksp. Teor. Fiz. **86**, 1784 (1984) [Sov. Phys. JETP. **59**, 1038 (1984)].

[15]S. Hikami, A. I. Larkin, and Y. Nagaoka, Prog. Theor. Phys. **63**, 607 (1980).

[16]B. L. Al'tshuler, A. G. Aronov, and D. E. Khmel'nitskii, Solid State Commun. **39**, 619 (1981).

[17]F. Komori, S. Kobayashi, and W. Sasaki, J. Phys. Soc. Jpn. **52**, 386 (1983).

[18]Y. Kawaguchi and S. Kawaji, Surf. Sci. **113**, 505 (1982).

[19]R. P. Taylor, M. L. Leadbeater, G. P. Whittington, P. C. Maan, L. Eaves, S. P. Beaumont, I. Mcintyre, S. Thomas, and C. D. W. Wilkinson, in *Proceedings of the Seventh International Conference on the Physics of Two-Dimensional Systems, Santa Fe, 1987*, edited by J. M. Worlock (North-Holland, Amsterdam, 1988), p. 52.

[20]H. Akaike, Ann. Inst. Statist. Math. **21**, 243 (1969); **21**, 407 (1969); T. J. Ulrych and M. Ooe, in *Nonlinear Methods of Spectral Analysis*, edited by S. Haykin (Springer-Verlag, Berlin, 1979).